Synthesis and Structural and Magnetic Characterization of Mixed Manganese−Copper $n = 1$ Ruddlesden−Popper Phases

E. E. McCabe and C. Greaves*

School of Chemistry, University of Birmingham, Birmingham B15 2TT, U.K.

Received July 17, 2006. Revised Manuscript Received August 16, 2006

New $n = 1$ Ruddlesden−Popper phases containing manganese and copper have been synthesized. Their structure has been investigated by X-ray and neutron powder diffraction and found to be tetragonal (*I*4/*mmm*) at temperatures down to 10 K. The series of materials $La_xSr_{2-x}Mn_{0.5}Cu_{0.5}O_4$ ($x = 0.75$, 1, 1.25, 1.5) displays significant Jahn−Teller distortions of the B site cations, with the degree of distortion increasing with x. The materials $LaSrMn_{0.5}Cu_{0.5}O_4$, $PrSrMn_{0.5}Cu_{0.5}O_4$, and $NdSrMn_{0.5}Cu_{0.5}O_4$ show interesting magnetic behavior with antiferromagnetic ordering, but evidence of some ferromagnetic interactions. $LaSrMn_{0.5}Cu_{0.5}O_4$ has long-range antiferromagnetic ordering and $La_{1.5}Sr_{0.5}Mn_{0.5}Cu_{0.5}O_4$ shows more complex behavior due to competing interactions, possibly resulting in a canted magnetic ground state.

Introduction

Ruddlesden−Popper (RP) phases are a class of layered perovskite related materials of general formula $A_{n+1}B_nO_{3n+1}$. They are composed of alternating rock salt and perovskite blocks, composed of n layers of corner linked BO_6 octahedra, stacked along the *c*-axis,[1,2] as shown in Figure 1. It is the layered nature of these materials which has led to significant interest in their electronic properties. A well-cited example is the $n = 2$ manganese containing material $La_{1.2}Sr_{1.8}Mn_2O_7$ which displays colossal magnetoresistance (CMR). This property is enhanced in this RP material due to its reduced dimensionality over the three-dimensional perovskite.[3]

The $n = 1$ manganese RP phases $La_{1-x}Sr_{1+x}MnO_4$ do not display CMR but nevertheless have been the focus of much research due to their unusual electronic structure.[4] The materials are antiferromagnetically ordered and $La_{0.5}Sr_{1.5}MnO_4$ also displays charge and orbital ordering.[5,6] The copper analogues $La_{2-x}A_xCuO_4$ have also received much attention and undergo interesting structural transformations as a function of temperature; the transitions are dependent on both x and the nature of the A cation.[7,8] The solid solution for which A = Sr also shows a range of interesting electronic properties from antiferromagnetic (AFM) insulating at low x to superconducting at $x = 0.15$ and to metallic at higher x.[9] Research has been carried out on the mixed manganese−copper perovskites, which are found to crystallize in orthorhombic or monoclinic symmetry and undergo distortions

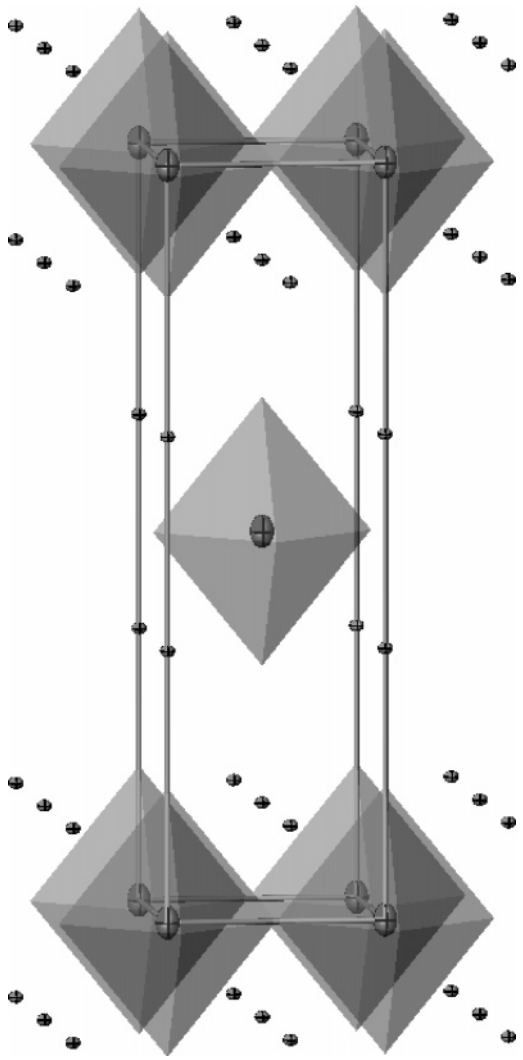

Figure 1. Unit cell of $n = 1$ RP material A_2BO_4 showing BO_6 octahedra and A cations.

* To whom correspondence should be addressed. E-mail: c.greaves@bham.ac.uk. Fax: 0121 414 4403.

(1) Ruddlesden, S. N.; Popper, P. *Acta Crystallogr.* **1957**, *10*, 538.
(2) Ruddlesden, S. N.; Popper, P. *Acta Crystallogr.* **1958**, *11*, 54.
(3) Moritomo, Y.; Asamitsu, A.; Kuwahara, H.; Tokura, Y. *Nature* **1996**, *380*, 141.
(4) Larochelle, S.; Mehta, A.; Lu, L.; Mang, P. K.; Vajk, O. P.; Kaneko, N.; Lynn, J. W.; Zhou, L.; Greven, M. *Phys. Rev. B* **2005**, *71*, 024435.
(5) Murakami, Y.; Kawada, H.; Tanaka, M.; Arima, T.; Moritomo, Y.; Tokura, Y. *Phys. Rev. Lett.* **1998**, *80* (9), 1932.
(6) Sternlieb, B. J.; Hill, J. P.; Wildgruber, U. C.; Luke, G. M.; Nachumi, B.; Moritomo, Y.; Tokura, Y. *Phys. Rev. Lett.* **1996**, *76* (12), 2169.
(7) Axe, D.; Moudden, A. H.; Hohlwein, D.; Cox, D. E.; Mohanty, M. K.; Moodenbaugh, A. R.; Xu, Y. *Phys. Rev. Lett.* **1989**, *62*, 2751.
(8) McAllister, J. A.; Attfield, J. P. *Phys. Rev. B* **2002**, *66*, 014514.

10.1021/cm061661j CCC: $33.50
Published on Web 10/31/2006

to rhombohedral symmetry, often as a function of oxygen nonstoichiometry.[10,11] However, little work has been carried out on the mixed manganese−copper $n = 1$ RP materials. We present here the synthesis and structural and magnetic characterization of the series $La_xSr_{2-x}Mn_{0.5}Cu_{0.5}O_4$, as well as $PrSrMn_{0.5}Cu_{0.5}O_4$ and $NdSrMn_{0.5}Cu_{0.5}O_4$.

Experimental Section

Polycrystalline samples of $Ln_xSr_{2-x}Mn_{0.5}Cu_{0.5}O_4$ (Ln = La, Pr, Nd) were prepared by the solid-state reaction of stoichiometric quantities of La_2O_3, Pr_6O_{11}, or Nd_2O_3, with $SrCO_3$, Mn_2O_3, and CuO (Aldrich, >99%). The reagents were intimately ground together and heated at 1250 °C either in air (for Ln = La and $x = 0.75$ and for Ln = La, Pr, Nd and $x = 1$) or in an atmosphere of flowing N_2(g) (Ln = La and $x = 1.25$, $x = 1.5$) for periods of 20 h with regular grinding. Room-temperature X-ray powder diffraction (XRPD) data were collected over a period of 10 h on a Siemens D5000 diffractometer (transmission mode, monochromated Cu $K\alpha_1$ radiation, step size of 0.0199°, position-sensitive detector). Constant wavelength neutron powder diffraction (NPD) data for $LaSrMn_{0.5}Cu_{0.5}O_4$ and $La_{1.5}Sr_{0.5}Mn_{0.5}Cu_{0.5}O_4$ were collected at 10 and 295 K on the powder diffractometer at NFL (Studsvik, Sweden) (λ = 1.47027 Å, double Cu monochromator). Room-temperature and 2 K TOF NPD data were collected for $PrSrMn_{0.5}Cu_{0.5}O_4$ and $NdSrMn_{0.5}Cu_{0.5}O_4$ at POLARIS (ISIS, U.K.). Rietveld structural refinements were carried out using the GSAS suite of programs.[12] Magnetic susceptibility was measured by ac excitation (amplitude 10 Oe) and by dc extraction (field of 2000 Oe) using a Quantum Design Physical Properties Measurements System. Thermogravimetric analysis (TGA) studies were carried out using a Rheometric Scientific STA, heating in 10% $H_{2(g)}$/90% $N_{2(g)}$ (to 1000 °C) and in $O_{2(g)}$ (to 800 °C). However, reduction was not a feasible way to assess oxygen stoichiometry as the samples decomposed to nonstoichiometric phases such as $La_{2-x}Sr_xCu_{1-y}Mn_yO_{4-\delta}$.

Results and Discussion

Structural Characterization from XRPD. Preliminary characterization of all materials was performed by Rietveld refinement of XRPD data. All materials were found to crystallize with body-centered tetragonal cells described by the ideal, high-symmetry space group *I*4/*mmm*, and there was no evidence to suggest distortions to lower symmetry. Traces of La_2O_3 were detected in $La_xSr_{2-x}Mn_{0.5}Cu_{0.5}O_4$ $x = 1.25$ and $x = 1.5$ samples and this was included in these refinements as a second phase. However, the La_2O_3 content refined to values of 0.21(2)% and 0.53(5)% by weight for the two samples and so is considered to have a negligible effect on the stoichiometry of the materials. All refinements showed a good fit between observed and calculated patterns and cell dimensions obtained from these refinements are given in Table 1.

Table 1. Table of Lattice Parameters from Refinement Using Room-Temperature XRPD Data for $La_xSr_{2-x}Mn_{0.5}Cu_{0.5}O_4$, $PrSrMn_{0.5}Cu_{0.5}O_4$, and $NdSrMn_{0.5}Cu_{0.5}O_4$

A site	$La_{0.75}Sr_{1.25}$ $x = 0.75$	LaSr $x = 1.00$	$La_{1.25}Sr_{0.75}$ $x = 1.25$	$La_{1.5}Sr_{0.5}$ $x = 1.50$	PrSr	NdSr
a/Å	3.81724(5)	3.81166(6)	3.79701(4)	3.79332(5)	3.79154)6)	3.78285(3)
c/Å	12.6599(1)	12.8173(2)	13.0298(1)	13.2075(1)	12.7167(2)	12.6584(1)
volume/Å^3	184.471(4)	186.220(5)	187.854(3)	190.046(4)	182.812(5)	181.141(2)

For the series $La_xSr_{2-x}Mn_{0.5}Cu_{0.5}O_4$, the increase in unit cell volume as the larger Sr^{2+} cation is replaced by La^{3+} is due to the reduction of the B site cations, from an average oxidation state of +3.25 for $x = 0.75$ to +2.5 for $x = 1.50$. The *c* parameter increases significantly while there is a small decrease in the *a* parameter. The decrease in unit cell volume as Pr^{3+} and Nd^{3+} replace La^{3+} on the A site is expected, due to the decrease in lanthanide cationic radius. These results are similar to the observations made by Hong et al.[13] of the pure manganese system, although in contrast to their study, these manganese−copper materials show a more isotropic decrease in unit cell parameters as a function of lanthanide cationic radius (possibly due to the absence of magnetic ordering of the lanthanide moments in these systems).

Structural Characterization from Room-Temperature NPD. Constant wavelength NPD data were collected at 295 K for $La_xSr_{2-x}Mn_{0.5}Cu_{0.5}O_4$ $x = 1$ and $x = 1.5$ samples and TOF NPD data were collected at 295 K for $PrSrMn_{0.5}Cu_{0.5}O_4$ and $NdSrMn_{0.5}Cu_{0.5}O_4$. Again, the diffraction patterns were consistent with *I*4/*mmm* symmetry and there was no evidence to suggest long-range ordering of the manganese and copper. Structural refinements were carried out using $Sr_{1.5}La_{0.5}MnO_4$[14] as a starting model and background parameters (linear interpolation), histogram scale factors, diffractometer zero points, peak shape, and atomic coordinates were refined. Fractional occupancies of the oxygen sites were refined, although they remained close to 1 and so most were fixed at the end of the refinement. This suggests that the materials are stoichiometric with respect to oxygen, unlike some pure copper $n = 1$ materials which contain oxygen vacancies.[15] Anisotropic thermal parameters were also refined, except for that for the B site in the low-temperature refinements which was constrained to be isotropic. These refinements (shown in Figure 2) were consistent with the trends in unit cell dimensions observed from the XRPD refinements. Details are given in Tables 2 and 3.

The bond lengths obtained reflect the Jahn−Teller (JT) distortions of the B site. The degree of distortion Δ_{JT} is given by the apical bond length divided by the equatorial bond length.[14] This distortion is approximately constant with temperature, but increases with *x* for the series $La_xSr_{2-x}Mn_{0.5}Cu_{0.5}O_4$. As the La^{3+} content increases and the B site cations are reduced, the concentration of JT active ions increases to a maximum for $x = 1.5$, with $La_{1.5}Sr_{0.5}Mn_{0.5}Cu_{0.5}O_4$ containing only JT ions Mn^{3+} and Cu^{2+} on the B site. Variations in the unit cell parameters with *x* are due to JT distortions of

(9) Radaelli, P. G.; Hinks, D. G.; Mitchell, A. W.; Hunter, B. A.; Wagner, J. L.; Dabrowski, B.; Vandervoort, K. G.; Viswanathan, H. K.; Jorgensen, J. D. *Phys. Rev. B* **1994**, *49* (6), 4163.
(10) Aldridge, S. A.; Battle, P. D.; Evans, J. S. O.; Moore, C. A.; Prior, T. J.; Wiseman, P. J. *Inorg. Chem.* **2005**, *44*, 197.
(11) Petrov, A. N.; Zuez, A. Y.; Tikchonova, I. L.; Voronin, V. I. *Solid State Ionics* **2000**, *129*, 179.
(12) Larson, A. C.; Dreele, R. B. v. *Los Alamos National Laboratory Report: LA-UR-86-748*; Los Alamos National Laboratory: Los Alamos, NM, 1987.
(13) Hong, C. S.; Chi, E. O.; Kim, W. S.; Hur, N. H.; Lee, K. W.; Lee, C. H. *Chem. Mater.* **2001**, *13*, 945.
(14) Bouloux, J. C.; Soubeyroux, J. L.; Daoudi, A.; Flem, G. L. *Mater. Res. Bull.* **1981**, *16*, 855.
(15) Nguyen, N.; Choisnet, J.; Hervieu, M.; Raveau, B. *J. Solid State Chem.* **1981**, *39*, 120.

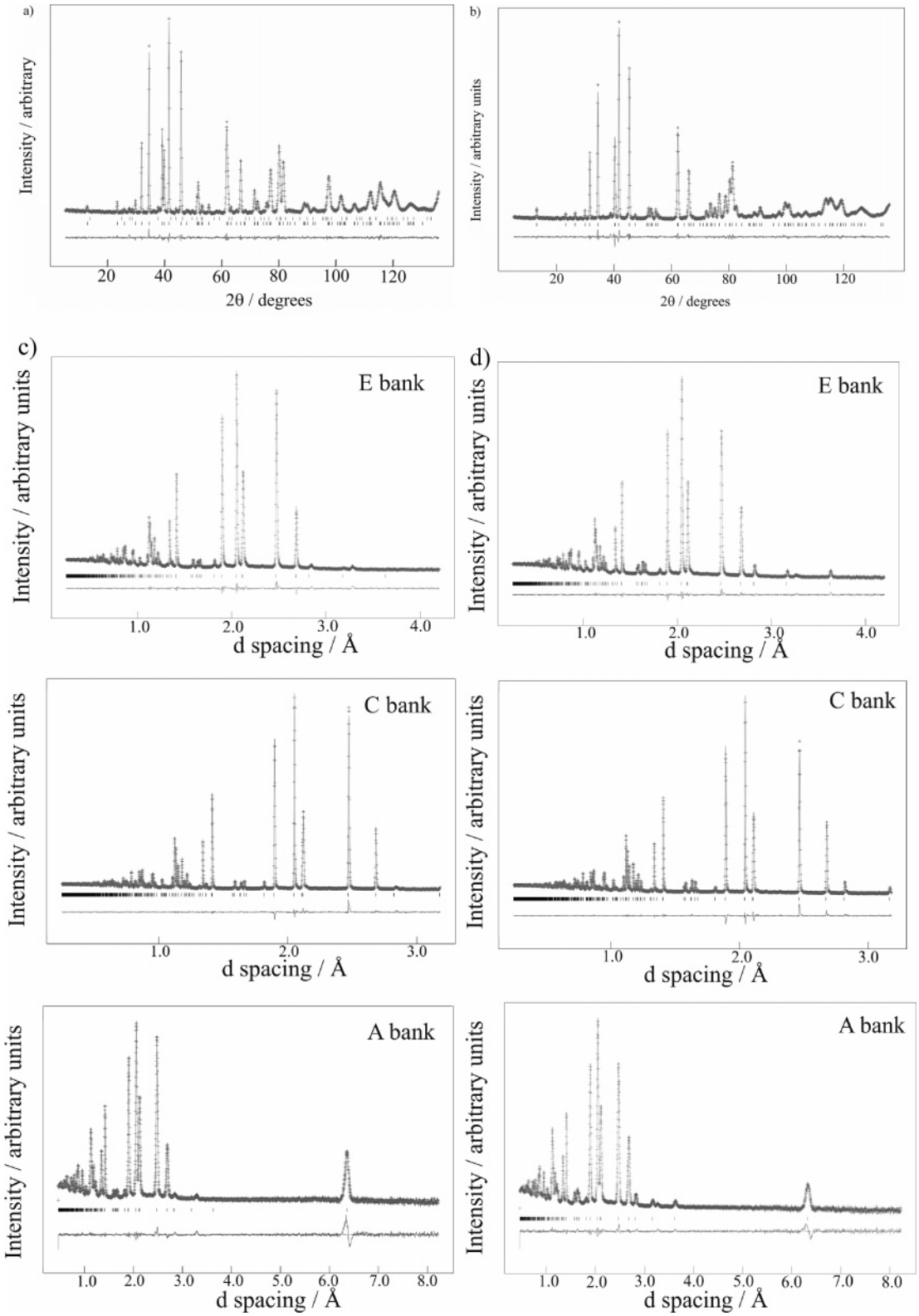

Figure 2. Observed (+), calculated, and difference NPD profiles (295 K data) of (a) $La_{1.5}Sr_{0.5}Mn_{0.5}Cu_{0.5}O_4$, $\chi^2 = 1.614$, $R_{wp} = 4.73\%$, $R_p = 3.60\%$, La_2O_3 content 1.78(9)% by weight, (b) $LaSrMn_{0.5}Cu_{0.5}O_4$, $\chi^2 = 1.896$, $R_{wp} = 5.02\%$, $R_p = 3.84\%$, (c) $PrSrMn_{0.5}Cu_{0.5}O_4$, $\chi^2 = 2.951$, $R_{wp} = 2.14\%$, $R_p = 1.69\%$, and (d) $NdSrMn_{0.5}Cu_{0.5}O_4$, $\chi^2 = 2.725$, $R_{wp} = 1.91\%$, $R_p = 1.62\%$, reflection positions of the main phase (and of La_2O_3) are marked (|) from bottom to top.

the B cations, as confirmed by the bond distances obtained from NPD refinements. Δ_{JT} shows little variation as the lanthanide A cation is substituted; this is expected as the B cation oxidation state (hence concentration of JT active cations) remains constant.

Comparison of the models obtained for the $La_xSr_{2-x}Mn_{0.5}Cu_{0.5}O_4$ $x = 1$ and $x = 1.5$ samples shows that a general feature of the $LaSrMn_{0.5}Cu_{0.5}O_4$ sample is of high U_{33} thermal parameters, reflecting increased motion of atoms along the [001] direction. This is noticeable for both A and B cation sites but more significantly for the apical oxygen site. In contrast, the $La_{1.5}Sr_{0.5}Mn_{0.5}Cu_{0.5}O_4$ model, while still showing some motion of the B cations along the [001] direction, shows much more isotropic motion of other cations and the

Table 2. Details from Refinements Using Room-Temperature NPD Data for $La_{1.5}Sr_{0.5}Mn_{0.5}Cu_{0.5}O_4$, $LaSrMn_{0.5}Cu_{0.5}O_4$, $PrSrMn_{0.5}Cu_{0.5}O_4$, and $NdSrMn_{0.5}Cu_{0.5}O_4$[a]

A site	$La_{1.5}Sr_{0.5}$	LaSr	PrSr	NdSr
a/Å	3.7927(1)	3.8154(2)	3.79161(8)	3.78285(4)
c/Å	13.2003(7)	12.8262(8)	12.7160(2)	12.6574(1)
A cation *z*	0.3585(1)	0.3593(1)	0.35815(2)	0.35874(1)
O(eq.) occupancy	1	0.986(6)	1	1
O(ap.) *z*	0.1776(1)	0.1674(1)	0.16840(9)	0.16815(3)
B−O(eq.)/Å	4 × 1.89635(9)	4 × 1.9077(1)	4 × 1.89581(4)	4 × 1.89143(2)
B−O(ap.)/Å	2 × 2.344(1)	2 × 2.147(2)	2 × 2.1413(4)	2 × 2.1284(4)
Δ_{JT}	1.236(1)	1.125(2)	1.1295(4)	1.1253(4)
R_{wp}/%	4.73	5.02	2.14	1.91
R_p/%	3.60	3.84	1.69	1.62
χ^2	1.614	1.896	2.951	2.725

[a] Refinements were carried out in space group *I*4/*mmm* with A cations on the 4e site (0, 0, *z*), B cations on 2a site (0, 0, 0), equatorial oxygens on the 4c site (0, 0.5, 0), and apical oxygens on the 4e site (0, 0, *z*).

Table 3. Anisotropic Thermal Parameters Obtained from Refinement Using 295 K NPD Data for (a) $La_{1.5}Sr_{0.5}Mn_{0.5}Cu_{0.5}O_4$, (b) $LaSrMn_{0.5}Cu_{0.5}O_4$, (c) $PrSrMn_{0.5}Cu_{0.5}O_4$, and (d) $NdSrMn_{0.5}Cu_{0.5}O_4$

atom	$U_{11} \times 100/Å^2$	$U_{22} \times 100/Å^2$	$U_{33} \times 100/Å^2$
	(a)		
La/Sr	0.73(5)	0.73(5)	0.48(7)
Mn/Cu	1.8(3)	1.8(3)	3.6(7)
O(eq.)	0.8(1)	0.1(1)	1.3(1)
O(ap.)	2.03(8)	2.03(8)	1.1(1)
	(b)		
La/Sr	0.71(7)	0.71(7)	1.22(9)
Mn/Cu	1.0(2)	1.0(2)	3.8(5)
O(eq.)	0.8(1)	0.3(1)	1.1(1)
O(ap.)	1.63(9)	1.63(9)	3.8(1)
	(c)		
Pr/Sr	0.748(7)	0.748(7)	0.73(1)
Mn/Cu	0.65(2)	0.65(2)	2.92(6)
O(eq.)	0.71(1)	0.51(1)	1.09(1)
O(ap.)	2.10(1)	2.10(1)	4.16(2)
	(d)		
Nd/Sr	0.791(6)	0.791(6)	0.636(9)
Mn/Cu	0.81(2)	0.81(2)	2.51(6)
O(eq.)	0.89(1)	0.56(1)	1.35(1)
O(ap.)	2.30(1)	2.30(1)	4.03(2)

O(ap.) site shows more motion in the *ab* plane, as expected for this structure. The models obtained for $PrSrMn_{0.5}Cu_{0.5}O_4$ and $NdSrMn_{0.5}Cu_{0.5}O_4$ also show high U_{33} thermal parameters for the O(ap.) site but the motion of the A site cations is much more isotropic. The high U_{33} thermal parameters observed from NPD refinements of this material are thought to reflect a degree of disorder due to the mixing of JT and non-JT ions in the structure. No ordering of the B cations is observed and so the B cation environment obtained from refinement of diffraction patterns is the average over the whole structure. This might explain the high degree of motion along the [001] direction as some B sites, containing JT cations, will be distorted, being elongated along the [001] direction leading to increased B−O(2)(ap.) bond lengths and influencing the A site position, while other B sites will contain non-JT cations and so will have undistorted octahedral environments. The models obtained for $PrSrMn_{0.5}Cu_{0.5}O_4$ and $NdSrMn_{0.5}Cu_{0.5}O_4$ also show high U_{33} thermal parameters for the apical oxygen site, consistent with a mix of Jahn−Teller and non-Jahn−Teller B cations, but the motion of the A site cations is much more isotropic. This is probably due to the significantly smaller cationic radii of Pr^{3+} and Nd^{3+} compared with that of La^{3+}. The volume of the 9-coordinate A site decreases slightly for this series of materials as the average A cation radius decreases.

Table 4. Details from Refinements Using Low-Temperature NPD Data for $La_{1.5}Sr_{0.5}Mn_{0.5}Cu_{0.5}O_4$ and $LaSrMn_{0.5}Cu_{0.5}O_4$ (Data Collected at 10 K) and $PrSrMn_{0.5}Cu_{0.5}O_4$ and $NdSrMn_{0.5}Cu_{0.5}O_4$ (Data Collected at 2 K)[a]

A site	$La_{1.5}Sr_{0.5}$	LaSr	PrSr	NdSr
a/Å	3.7847(1)	3.8058(1)	3.77956(3)	3.77392(2)
c/Å	13.1766(6)	12.8151(7)	12.6916(2)	12.6385(1)
A cation *z*	0.3587(1)	0.3592(1)	0.35795(2)	0.35865(1)
O(eq.) occupancy	1	0.984(6)	1	1
O(ap.) *z*	0.1776(1)	0.1673(1)	0.16833(4)	0.16816(3)
B−O(eq.)/Å	4 × 1.89233(8)	4 × 1.90287(9)	4 × 1.88978(2)	4 × 1.88696(1)
B−O(ap.)/Å	2 × 2.340(1)	2 × 2.144(2)	2 × 2.1364(5)	2 × 2.1253(4)
Δ_{JT}	1.237(1)	1.127(2)	1.1305(4)	1.1263(4)
moment on Mn/μ_B	±2.559(3)	±0.92(9)	±0.5(1)	±0.77(5)
moment on Cu/μ_B	±0.640(3)	±0.31(3)	±0.17(5)	±0.26(1)
R_{wp}/%	5.19	5.29	1.39	1.17
R_p/%	3.94	4.00	2.59	1.67
χ^2	1.953	2.093	2.381	9.447

[a] Refinements were carried out in space group *I*4/*mmm* with A cations on the 4e site (0, 0, *z*), B cations on the 2a site (0, 0, 0), equatorial oxygens on the 4c site (0, 0.5, 0), and apical oxygens on the 4e site (0, 0, *z*). The overall moment on the B site was refined and attributed to manganese and copper cations according to the constraints described in the text.

Structural Characterization from Low-Temperature NPD. Refinements using the low-temperature data revealed structural features similar to those found from the 295 K refinements and refinement details are given in Table 4. However, these low-temperature patterns were found to contain extra peaks that could not be indexed by the structural cell. These are particularly noticeable at low angles (see Figure 3), especially for $La_{1.5}Sr_{0.5}Mn_{0.5}Cu_{0.5}O_4$. The first three peaks were indexed as the [100], [101], and [012] reflections of an enlarged unit cell of dimensions $\sqrt{2}a \times \sqrt{2}a \times c$; this cell was found to index all magnetic peaks observed and was consistent with the lower intensity peaks observed for $LaSrMn_{0.5}Cu_{0.5}O_4$, $PrSrMn_{0.5}Cu_{0.5}O_4$, and $NdSrMn_{0.5}Cu_{0.5}O_4$. A magnetic phase was therefore included in the refinement with moments of nearest neighbor B cations aligned antiferromagnetically within the perovskite layers. From refinements, the best model had moments aligned along the [001] direction and refined moments are given in Table 4. Constraints were applied to the magnitudes of the moments on manganese and copper cations, based on the expected number of unpaired electrons on each metal (for $La_{1.5}Sr_{0.5}Mn_{0.5}Cu_{0.5}O_4$ containing Mn^{3+} (d^4) and Cu^{2+} (d^9), the moment on manganese sites was constrained to be 4 times that on the copper sites; for $LaSrMn_{0.5}Cu_{0.5}O_4$, $PrSrMn_{0.5}Cu_{0.5}O_4$, and $NdSrMn_{0.5}Cu_{0.5}O_4$ containing an average B cation oxidation state of +3, which is assumed to be due to Mn^{4+} (d^3) and Cu^{2+} (d^2), the moment on manganese sites was constrained to be 3 times that on the copper sites). Figure 4 shows the relationship between the magnetic cell and the nuclear cell and the arrangement of magnetic moments in the structure. However, there are very few magnetic peaks, with low intensity, and although a good fit was obtained with this simple model, there are other models that might describe the magnetic structure of these materials, as described below. The moments obtained for the manganese and copper sites

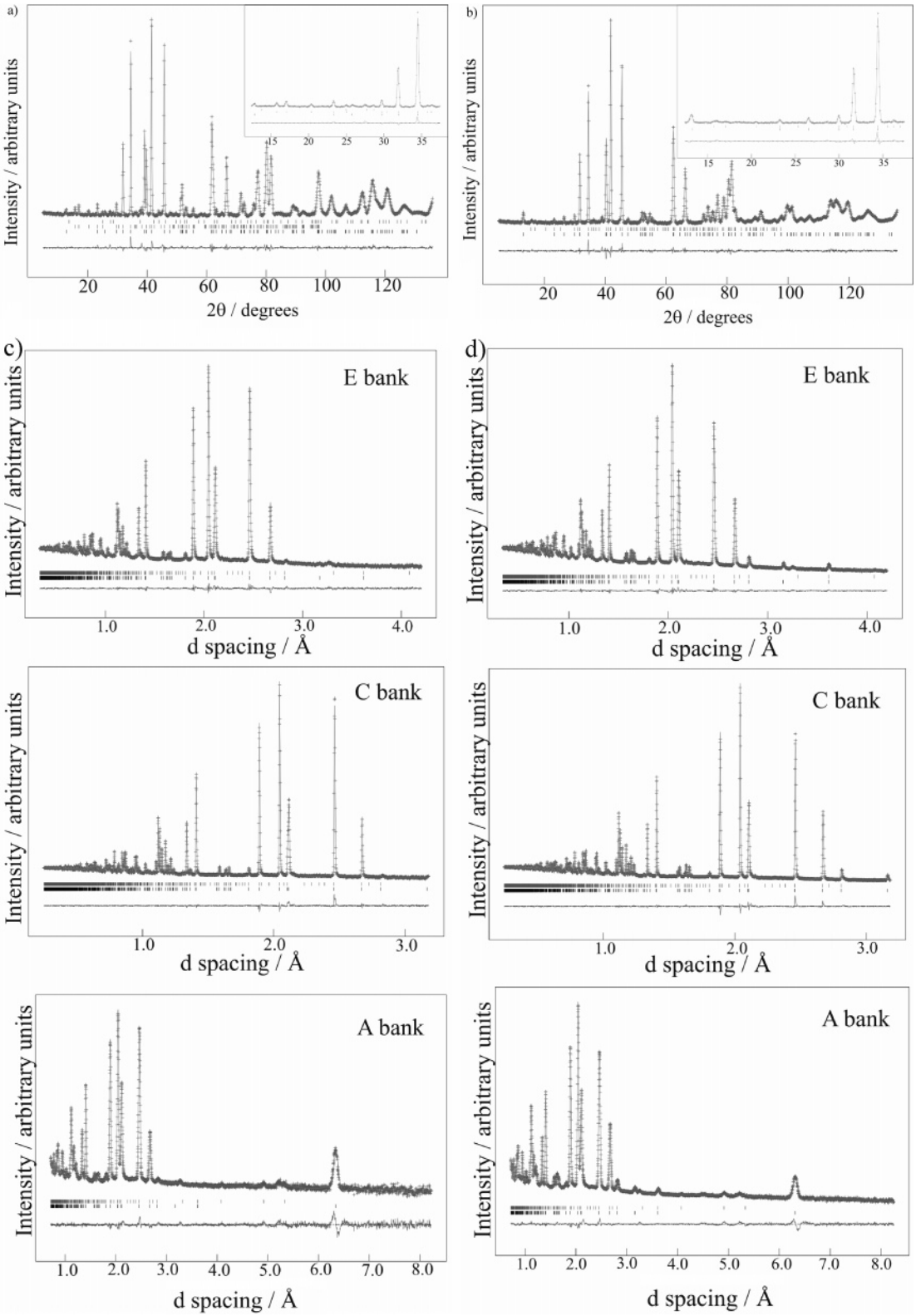

Figure 3. Observed (+), calculated, and difference NPD profiles (low-temperature data) of (a) $La_{1.5}Sr_{0.5}Mn_{0.5}Cu_{0.5}O_4$, $\chi^2 = 1.953$, $R_{wp} = 5.19\%$, $R_p = 3.94\%$, La_2O_3 content 1.54(9)% by weight, (b) $LaSrMn_{0.5}Cu_{0.5}O_4$, $\chi^2 = 2.093$, $R_{wp} = 5.29\%$, $R_p = 4.00\%$, (c) $PrSrMn_{0.5}Cu_{0.5}O_4$, $\chi^2 = 2.381$, $R_{wp} = 1.39\%$, $R_p = 2.59\%$, (d) $NdSrMn_{0.5}Cu_{0.5}O_4$, $\chi^2 = 9.447$, $R_{wp} = 1.17\%$, $R_p = 1.67\%$, reflection positions of the main phase and magnetic phase (and of La_2O_3) are marked (|) from bottom to top.

from refinements are lower than might be expected for these ions, which is attributed to incomplete ordering of the moments as is often observed in layered materials.

Magnetic Characterization of $La_{1.5}Sr_{0.5}Mn_{0.5}Cu_{0.5}O_4$. Figure 5 shows the magnetic susceptibility of $La_{1.5}Sr_{0.5}MnO_4$. There is a plateau in the susceptibility centered around $T =$ 93 K, but it should be noted that there is also a change in gradient at ~280 K. The inverse susceptibility (shown in the inset in Figure 5) does not vary linearly with temperature, suggesting that the material does not behave as a Curie−Weiss paramagnet in the temperature range studied. These measurements suggest that the magnetic behavior of this

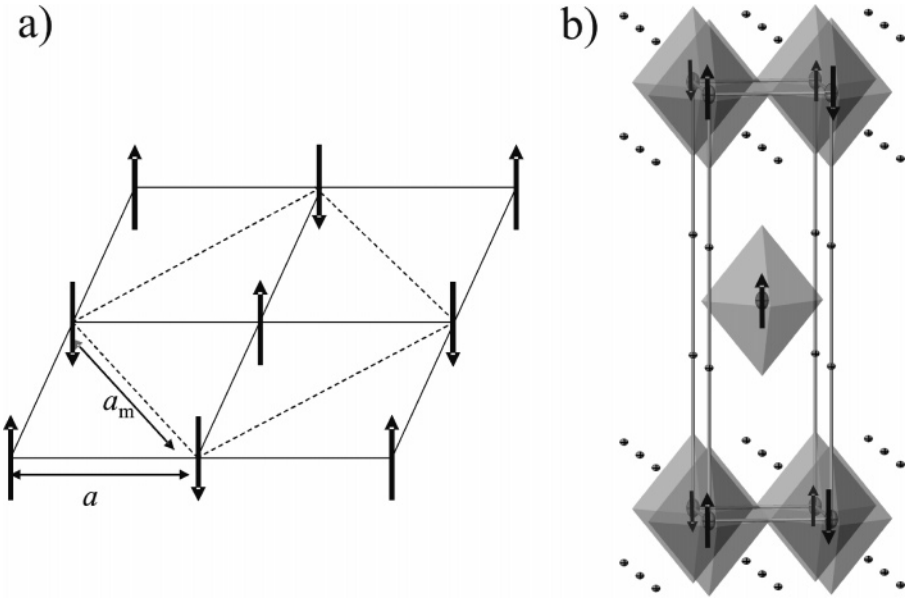

Figure 4. (a) Relationship between magnetic (---) and nuclear (−) unit cell and (b) arrangement of moments represented by black arrows, within structure. This magnetic structure has been observed from NPD data for all materials described here.

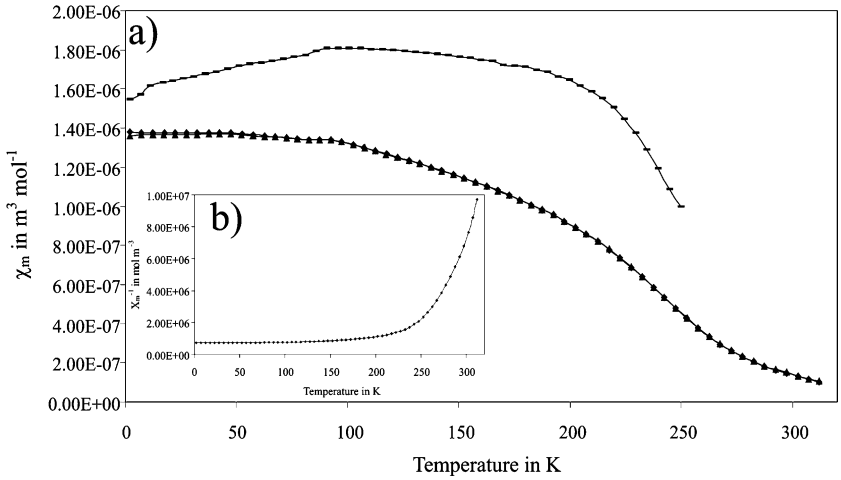

Figure 5. (a) Magnetic susceptibility versus temperature plot of $La_{1.5}Sr_{0.5}Mn_{0.5}Cu_{0.5}O_4$ in applied field of 2000 Oe, ACMS data collected with amplitude 10 Oe, and inset (b) inverse susceptibility versus temperature plots, ZFC (▲), FC (◆), and ACMS (−) data shown.

material is complex. The gradient of the susceptibility versus temperature plot at ∼280 K and the observation of a broad maximum may reflect some ferromagnetic interactions, possibly resulting in canting of the moments. Canting could arise as a result of competing interactions. Exchange interactions between the empty d_{x2-y2} orbital on the JT Mn^{3+} cation and the half-filled d_{x2-y2} orbital on the JT Cu^{2+} cation would result in FM coupling. However, $Mn^{3+}-Mn^{3+}$ and $Cu^{2+}-Cu^{2+}$ exchange interactions would lead to AFM ordering. If the relative strengths of the FM $Mn^{3+}-Cu^{2+}$ and AFM $Mn^{3+}-Mn^{3+}/Cu^{2+}-Cu^{2+}$ interactions change with temperature, the observed change in susceptibility with temperature might be explained. If the FM interactions dominate at higher temperatures but the AFM coupling increases in strength on cooling, this could lead to a ground state with canted spins, which satisfies both these competing interactions to an extent.

Magnetic Characterization of $LnSrMn_{0.5}Cu_{0.5}O_4$ (Ln = La, Pr, Nd). Figure 6 shows the variation of magnetic susceptibility with temperature for $LaSrMn_{0.5}Cu_{0.5}O_4$. There is a maximum at $T_N = 87$ K, again suggesting AFM ordering. The plot of inverse susceptibility versus temperature (see inset to Figure 6) shows Curie−Weiss behavior above this ordering temperature, but with two regions of differing gradient. Application of the Curie−Weiss law gives positive Weiss constants for both slopes, and the paramagnetic moment increases from 2.27 μ_B at $T > 215$ K to 2.99 μ_B at $100 \text{ K} < T < 215$ K. The theoretical paramagnetic moment of a mixed $Mn^{4+}-Cu^{2+}$ system is 3.00 μ_B, while that of a mixed $Mn^{3+}-Cu^{3+}$ is higher (4.00 μ_B for high-spin Cu^{3+}) and so the observed paramagnetic moment is more consistent with a mixed $Mn^{4+}-Cu^{2+}$ system, particularly at low temperatures. The presence of two regions in the inverse susceptibility plot may signify two types of magnetic interactions, favored at different temperatures. From the positive Weiss constants, both slopes are consistent with FM interactions and the moment increases on cooling. FM coupling could arise from either superexchange or double-exchange interactions between the empty d_{x2-y2} Mn^{4+} orbital and the half occupied d_{x2-y2} orbital on the JT distorted Cu^{2+} cation. However, the maximum in susceptibility at 87 K is indicative of AFM coupling within the perovskite layers. NPD gives no evidence of long-range ordering of manganese

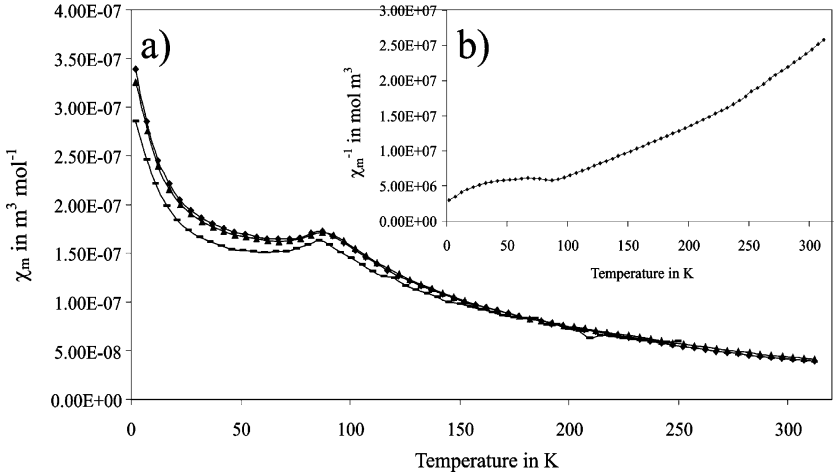

Figure 6. (a) Magnetic susceptibility versus temperature plot of $LaSrMn_{0.5}Cu_{0.5}O_4$ in applied field of 2000 Oe, ACMS data collected with amplitude 10 Oe, and inset (b) inverse susceptibility versus temperature plots, ZFC (▲), FC (◆), and ACMS (−) data shown.

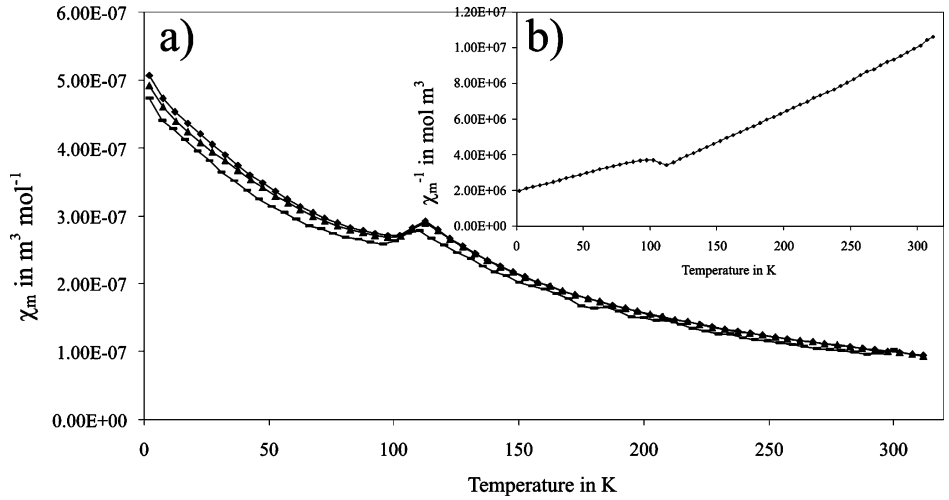

Figure 7. (a) Magnetic susceptibility versus temperature plot of $PrSrMn_{0.5}Cu_{0.5}O_4$ in applied field of 2000 Oe, ACMS data collected with amplitude 10 Oe, and inset (b) inverse susceptibility versus temperature plots, ZFC (▲), FC (◆), and ACMS (−) data shown.

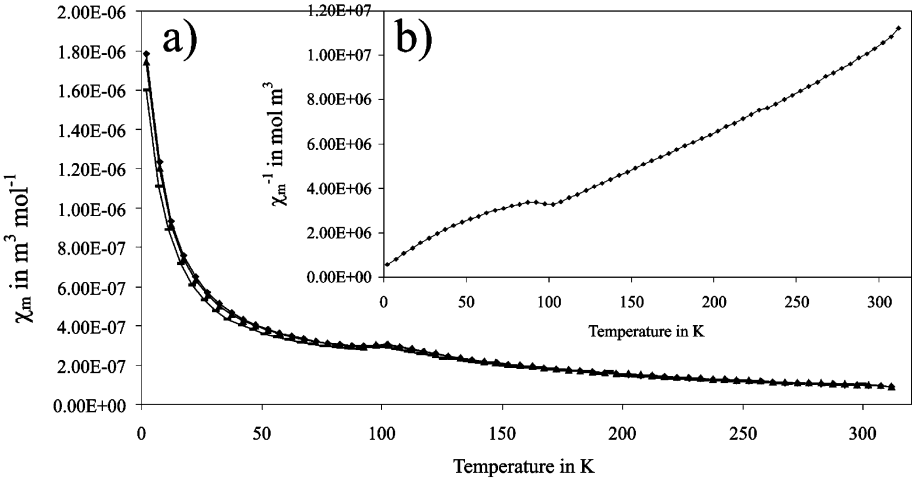

Figure 8. (a) Magnetic susceptibility versus temperature plot of $NdSrMn_{0.5}Cu_{0.5}O_4$ in applied field of 2000 Oe, ACMS data collected with amplitude 10 Oe, and inset (b) inverse susceptibility versus temperature plots, ZFC (▲), FC (◆), and ACMS (−) data shown.

and copper and $Mn^{4+}-Mn^{4+}$ and $Cu^{2+}-Cu^{2+}$ exchange interactions would give rise to AFM ordering within layers. Nevertheless, it is possible that small FM clusters of manganese and copper exist, these clusters being aligned antiferromagnetically with one another. Susceptibility measurements for $PrSrMn_{0.5}Cu_{0.5}O_4$ and $NdSrMn_{0.5}Cu_{0.5}O_4$ (see Figures 7 and 8) are qualitatively very similar to that observed for $LaSrMn_{0.5}Cu_{0.5}O_4$. Both materials show a maximum in susceptibility, indicating AFM ordering. The ordering temperatures are similar to that found for $LaSrMn_{0.5}Cu_{0.5}O_4$ ($T_N = 112$ K for $PrSrMn_{0.5}Cu_{0.5}O_4$, $T_N = 102$ K for $NdSrMn_{0.5}Cu_{0.5}O_4$, compared with $T_N = 87$ K for $LaSrMn_{0.5}Cu_{0.5}O_4$), suggesting that the nature of the lanthanide cation has little influence on the magnetic ordering of these

materials. Above the ordering temperature, the inverse susceptibility of both samples varies linearly with temperature and the Curie−Weiss paramagnetic moment calculated is significantly higher than that observed for $LaSrMn_{0.5}Cu_{0.5}O_4$, but very similar for both these materials ($\mu_{eff} = 4.24\ \mu_B$ for both, compared with theoretical values of 4.67 μ_B and 4.70 μ_B for $PrSrMn_{0.5}Cu_{0.5}O_4$ and $NdSrMn_{0.5}Cu_{0.5}O_4$ respectively, assuming that the B site is occupied by Mn^{4+} and Cu^{2+}). The increased paramagnetic moment in these two samples is due to the magnetic moments on the lanthanide cations incorporated onto the A site. Again, these samples have positive Weiss constants ($\theta = 18.61$ K for $PrSrMnO_4$, $\theta = 1.43$ K for $NdSrMnO_4$), suggesting some ferromagnetic interactions. These measurements suggest that the magnetic behavior of $LnSrMn_{0.5}Cu_{0.5}O_4$ is very similar for Ln = La, Pr, Nd, with the lanthanide cation not influencing the magnetic ordering. This is in contrast to the system $Nd_{0.5}Sr_{1.5}MnO_4$, in which the moments on the Nd^{3+} cation order at 21 K.[13] The absence of magnetic ordering on the lanthanide sublattice in these mixed manganese−copper systems may be a result of the increased disorder of the system. The disorder of Ln and Sr over the A sites, coupled with the disorder of manganese and copper over the B site in these materials, would lead to a very varied local environment for the lanthanide cations and would perhaps reduce their tendency to order.

B Cation Oxidation State in $LnSrMn_{0.5}Cu_{0.5}O_4$. These $LnSrMn_{0.5}Cu_{0.5}O_4$ (Ln = La, Pr, Nd) materials have an average B cation oxidation state of +3 and could contain either $Mn^{3+}-Cu^{3+}$, $Mn^{4+}-Cu^{2+}$, or a mixture of both combinations. From consideration of bond lengths, it is difficult to differentiate between the three possible combinations. The observed degree of Jahn−Teller distortion is perhaps more consistent with $Mn^{4+}-Cu^{2+}$, rather than $Mn^{3+}-Cu^{3+}$.[9,14,16,17] This is consistent with the chemistry of related systems. Fluorination studies of $LaSrMnO_4$ and La_2CuO_4 would also suggest that the oxidation of Mn^{3+} to Mn^{4+} is a more facile process than that of Cu^{2+} to Cu^{3+}: fluorination of $LaSrMnO_4$ gives $LaSrMnO_4F_{1.7}$ as the fully fluorinated product with a manganese oxidation state of +4.7,[18] while the maximum fluorine content of the copper analogue is much lower, the fully fluorinated product being $La_2CuO_4F_{0.41}$ with a copper oxidation state of +2.41.[19] The Curie−Weiss paramagnetic moment obtained for $LaSrMn_{0.5}Cu_{0.5}O_4$ also supports this conclusion.

Conclusions

In conclusion, we present here the synthesis and structural and magnetic characterization of the $n = 1$ RP series $La_xSr_{2-x}Mn_{0.5}Cu_{0.5}O_4$ for $x = 0.75$, 1, 1.25, and 1.5 as well as $PrSrMn_{0.5}Cu_{0.5}O_4$ and $NdSrMn_{0.5}Cu_{0.5}O_4$. Rietveld analysis of XRPD data indicates that the materials exhibit significant Jahn−Teller distortions which become more pronounced with increasing La^{3+} content and this is confirmed by bond lengths obtained from Rietveld analysis of NPD data. The materials $LnSrMn_{0.5}Cu_{0.5}O_4$ (Ln = La, Pr, Nd) are believed to contain Mn^{4+} and Cu^{2+} ions and magnetic measurements suggest some evidence of FM interactions at higher temperatures, before long-range AFM ordering is observed on cooling. $La_{1.5}Sr_{0.5}Mn_{0.5}Cu_{0.5}O_4$ displays more complex magnetic behavior; the susceptibility goes though a broad maximum and may indicate a canted arrangement of moments due to competing FM interactions which dominate at higher temperatures, and AFM interactions which increase in strength on cooling.

Acknowledgment. We thank EPSRC for financial support and the NFL for the provision of neutron diffraction facilities. We are grateful to Dr. H. Rundlöf and Dr. R. Smith for experimental assistance with the collection of NPD data.

CM061661J

(16) Rial, C.; Moran, E.; Alario-Franco, M. A.; Amador, U.; Andersen, N. H. *Physica C* **1997**, *288*, 91.
(17) Goodenough, J. B.; Demazeau, G.; Pouchard, M.; Hagenmuller, P. *J. Solid State Chem.* **1973**, *8*, 325.
(18) Aikens, L. D.; Li, R. K.; Greaves, C. *Chem. Commun.* **2000**, 2129.
(19) Chevalier, B.; Tressaud, A.; Lepine, B.; Robin, C.; Etourneau, J. *J. Less Common Met.* **1990**, *164−165*, 832.